

## **FULL AUTOMATIZATION OF WATERJET CUTTING**

M. Bauer, O. Grünzel, H. J. Maier, T. Hassel

Institut für Werkstoffkunde (Materials Science), Leibniz Universität Hannover, Germany

### **ABSTRACT**

Many costs for waterjet cutting are caused by limited lifetime of components such as orifices or focusing tubes. Today, defective orifice or the focusing tube are detected by the machine operators upon process failure. Early detection of an imminent failure of these components requires an experienced machine operator. Most of the time, however, one can only distinguish between a functional tool and a damaged tool. For a full automatization of a waterjet cutting system, a reliable indicator of damage is needed.

In this study, the wear parameters and their influence on the failure of orifices and focusing tubes were investigated. At first the damage state of the components (orifice and focusing tube) was analyzed by using light imaging and laser confocal microscopy. In the present water jet cutting process four components (damaged/new orifice and damaged/new focusing tube) were observed with a high-speed camera and analyzed by thermography and acoustic emission. After the evaluation of all data, damage of the orifice and/or the focusing tube could be identified with a high reliability. Next, the focus was set on the automatization of the water jet cutting head. Therefore a high pressure screw connection was designed. With this smart tool it is possible cutting to change a cutting head between pure water, abrasive water injection jet (AWIJ) and abrasive water suspension jet (AWSJ). In connection with the idea of process observing in a full automatized mode becomes feasible.

## **1. INTRODUCTION**

Nowadays, many processes like milling or drilling are monitored. If incoming events are detected, they are resolved accordingly. In waterjet applications, the machine operators detect damages of tool parts in the area of the cutting head. Currently there is no online monitoring tool for the wear of the orifice or the focusing tube. Most of the previous studies focus on - focusing tube wear. The most important reasons for replacement of the focusing tubes are that they are worn (85%) or broken (13 %). Thus, the wear of the focusing tube is a significant factor of the abrasive water-jet machining. Worn of the focusing tubes influence the cut geometry as well as the surface quality [MOM98]. The most common method to estimate the focusing tube wear is by measuring the focus outlet diameter over a given period. In the year 1994 Mohamed Hashish [HAS94] made a study about the inner diameter of focusing tubes and the correlation between focusing tube material and wear. He showed data suggesting that the wear mechanisms along the mixing tube change from erosion by particle impact at the upstream sections to abrasion at the downstream sections [HAS94]. This study shows also a dependency of the orifice diameter on the focus wear. In addition, Kovacevic et al. [KOV89] address in their study that wear rate increases with an increase in the abrasive mass flow rate. In a further investigation Kovacevic et al. [KOV94] analyzed the relationship between the nozzle inside diameter and the generated acoustic signal. They installed a microphone next to the waterjet machine and monitored the process noise during material cutting and without cutting. A change in the level of the acoustic signal could be detected. Also the orifice was observed as critical parameter. A misalignment with the focusing tube or a microscopic chip in an orifice can reduce nozzle life to minutes instead of hours [KOV94]. Their conclusion is that the conventional FFT method gives an unrealistic assumption about the data. They state that is difficult to extract useful characteristics out of the time series based on the assumption that the signal is made up of sine and cosine waves with different frequencies. Therefore, the analysis it is more estimations than defined statements about the state of components.

This study is to investigate the correlation between the orifice/focusing tube wear and a controlling system. For this, high speed recordings, thermographic emission and acoustic emission of the mixing chamber and the hole cutting head were carried out. The aim was to investigate which experimental methods give the most or the best information about the wear of orifice and focusing tube. In addition, an automated connection of the cutting head is explained.

## **2. MATERIALS AND METHODS**

### **2.1 MATERIALS**

#### **2.1.1 Experimental setup**

For all experiments a high pressure intensifier (BFT GmbH, Type Servotron 40.37) with a maximum pressure of 400 MPa and a maximum flow rate of 3.8 l/min was used. The cutting table consisted of a catcher (2000x1000mm), a controlled X/Y axis and a manual Z axis. The valves and the abrasive dosing system were numerical controlled by a NC control system (Baldor GmbH).

Garnet Mesh #120 (GMA Garnet Europe GmbH) was employed as the abrasive particle for all tests (see Table 1). The used cutting head (BFT GmbH) is shown at Figure 5.

### **2.1.2 Orifice**

The used orifices were of the type sapphire 1830 (Comadur Sa) with a diameter of 0.3 mm. At the beginning of the investigation two orifices were selected. One brand new one and one orifice, which ran more than 60 hours. These were the starting conditions. Within the experiments both orifices got worn for about 10 more hours. The state of both orifices were analyzed at the beginning of the experiments by using light microscopic imaging. Figure 1a shows the top and Figure 1b the bottom of the damaged orifice. Both the top and the bottom has significant outbreaks in the sapphire. The diameter of the orifice at the bottom is 0,321 mm and maximum of diameter at the outbreaks is about 2,5 mm. In comparison, the brand new orifice has a diameter at the bottom of 0,301 mm and is shown in Figure 1c & 1d.

To get more information about the outbreaks at the top, the orifices were pictured with a laser confocal microscope (Figure 2). The image shows an uneven surface of the entry radius of the used orifice in Figure 2a. Also the drilling hole is slightly oval in the middle of the sapphire. In comparison, Figure 2b show a perfect concentric entry to the hole of the orifice.

### **2.1.3 Focusing tube**

The focusing tubes in this study were of type Roctec 100 (Kennametal, GMA Garnet Europe GmbH) and had the dimensions of 6.00x0.8x70mm (Outside diameter, inside diameter, length). The material of this tubes is Roctec 100 which has a high Vickers hardness of about 25.5-27.7 kg/mm<sup>2</sup> [KEN17]. The starting conditions were the same as for the orifices. One brand new one, one with a run time of more than 60 hours and both got about 10 hours of wear during the experiments. The light microscope images - are displayed in Figure 3. Figure 3a shows the top and 3b the bottom of the damaged focusing tube. This tube had a diameter of 1.01 mm at the outlet side. In the inlet, this tube was washed out. Because of the depth it was not possible to picture the inlet radius with light microscope imaging or laser confocal microscopy. The new focusing tube is shown in Figures 3c-d. This had an inner diameter of 0.803 mm at the beginning of the experiments.

## **2.2 METHODS & IMPLEMENTATION OF EXPERIMENTS**

In all experiments of present water jet cutting process four variation of experimental setup (see Table 2) were observed with the following methods. The cutting head is stationary during the entire test. Thus the measured results are not influenced by vibrations of the machine axis.

### **2.2.1 High speed camera**

For the visual detection of defects of the orifice or the focusing tube the high-speed camera Photron Fastcam SA5 (Photron USA Inc., San Diego, USA) was used. This camera delivers excellent light sensitivity (ISO 10000-test). The dynamic range through is a 12-bit monochrome sensor with twenty micron square pixels and had a memory flash of 8 Gb. In the experiments the water jet stream was recorded with a resolution of 256 pixels x 1024 pixels and a bit rate of 500 fps. This

corresponds to one picture every 2 ms. The recording time was about 5 seconds, which was chosen because the system becomes homogenous right after the valve opened. The observed area is illuminated from one side using an infrared laser (Cavilux HF, Fa. Acal BFi Germany GmbH, Gröbenzell, Germany) with a frequency equal to the frame rate of 500 fps.

### 2.2.2 Thermography emission

To analyze the heat up of defect components, the cutting head's temperature was measured using thermography emission camera type ThermaCam SC3000 (FLIR Systems, Wilsonville, Oregon, USA). The image recording frequency was set to 10Hz with a resolution of 404 pixels  $\times$  240 pixels. For all measurements, the cutting head's surface was blackened using a graphite spray prior to the experiment to obtain a constant coefficient of emission of  $\alpha=0.95$ . After measuring, the temperature at the three positions safety screw, focusing tube, and mixing chamber (see Figure 5) were evaluated with the software ThermaCam Researcher Pro 2.7 (FLIR Systems, Wilsonville, Oregon, USA).

### 2.2.3 Acoustic emission

Another method to get information if orifice or focusing tube are damaged is to analyze the cutting head's acoustic emission. Therefore, the acoustic emission sensor was mounted on the cutting head. The position was opposite to the abrasive inlet (see Figure 5).

The measurement data for the acoustic emission was acquired with a Deci SE650-P AE sensor. This sensor type is charge based and delivers an extremely small currents output. Therefore a charge amplifier was used. The employed amplifier is a Vallen AEP4 (Vallen Systeme GmbH, Icking, Germany) with a Bandwidth of 2.5 kHz to 1 MHz. As coupling media between sensor and cutting head surface Äronix Siliconfett (ÄRONIX Spezialschmierstoffe, Walldorf, Germany) was used. The measurement was taken with a NI 6133 device (National Instruments, München, Germany) at 2 MS/s sampling rate with a length of 5 seconds for every single combination of pressure, orifice and nozzle. This was done with a Python3 script interfacing the National Instruments device driver. To ensure a high enough writing throughput during measurement the data was written onto the hard disk as raw 16bit binary file.

All analysis was performed afterwards. The measurement data was decoded from binary to a structured time series format by using an R based software algorithm. After data conversion the first  $N = 50.000$  data points of every measurement file were used to perform a Fast Fourier transformation (FFT) to determine characteristic frequencies for specific operating conditions of the waterjet. The FFT was calculated according to the following formula [COO65]

$$a_k = \sum_{j=0}^{2^n-1} a_j \cdot \omega^{j \cdot k} \quad (k = 0, \dots, 2^n - 1)$$

Data conversion and analysis require a significant amount of calculation time. Time needed to convert the data can only be shortened by using a faster computer or reducing the measurement time or respectively the number of data points used in the analysis. Reducing measurement time would limit the ability to perform in depth analyses of the existing data with other methods later on. The discrete Fourier transformation has a complexity of

$$FFT \in \mathcal{O}(N \log(N))$$

meaning that calculation time increases nonlinear with an increasing number of data points used in the analysis [VET84]. The minimal detectable frequency difference depends on the number  $N$  of data points analyzed following the formula

$$f_{\text{resolution}} = \frac{\text{sampling rate}}{2 \cdot N}$$

Better frequency resolution can only be archived by using more data points when performing the FFT. It has to be considered that the upper limit of frequencies that can be analyzed is half of the used sampling rate of data acquisition according to stability criterion of Nyquist. The parameters used in the shown analyses therefor allow a frequency resolution with a 80 Hz step width [KAM02].

For further data analysis wavelets are a promising option because this method would allow time based frequency analysis for the process. If characteristic frequencies can be linked to certain operational states the Goertzel algorithm is an option to develop a cost effective online monitoring system for the waterjet cutting head [BEC01, GEN69].

#### **2.2.4 Design of an automated high pressure screw connection tool**

With a tool monitoring system as described above (2.2.3) it is possible to get the information about the wear of the orifice and the focusing tube. Thus, the next step for fully automatic waterjet cutting is an automated high-pressure screw connection. For this purpose an adapter was designed, which allows it to be sealed tightly with the collimating tube. The angle of the adapter's cone is lower than the of the collimating tube's cone. The sealing surfaces of both parts don't get fretted, because the adapter is guided linear. Due to the different thread pitch of the adapter and the guided locking screw, the adapter is pulled linearly from the bottom to the top without any other support. In order to always find the first thread, the adapter is mounted with springs. In the event that the first thread is not hit the first time, the adapter is pressed down. The counterforce of the springs pushes the apex upwards and thus increases the probability of the threaded engagement in the second rotation of the screw. The tightness of the connection is ensured by a high tightening torque ( $>60$  Nm). This high tightening torque is generated by a stepping motor and worm gear with a transmission ratio of 1:11.25. Just the same way the connection is tightened it can also be loosened again by reversing the process. In this design (see Figure 12), the bottom of the adapter has an M12 thread and is designed like a conventional collimating tube. This allows any types of cutting head to be adapted with an M12 thread. Together with a turntable tool revolver or a tool bar the cutting heads can be changed within seconds between pure water jet, abrasive water injection jet (AWIJ) and abrasive water suspension jet (AWSJ). For cutting with abrasive water suspension jet, however, a special valve is required, which is described in publication of Bauer et al. [BAU14] and in patent application DE102014100839B4.

### **3. RESULTS**

#### **3.1 High speed recordings**

The trial E1 shows a very homogenous abrasive waterjet injection jet (AWIJ) with a stream diameter of approximately 1mm in the observed range of 30 mm after the focusing tube outflow (Figure 4). By comparison, E2 manifests that the AWIJ expands directly after the focusing tube exit. The diameter of the AWIJ reaches nearly 3mm. This behavior could also be detected in trial E4. There is not significant difference by optical observation. Trial E2 has a new focusing tube and E4 a damaged one. In both trials the orifice is damaged. Only the state of the focusing tube changes from new (E2) to damaged (E4). Thus, it is not possible to visually determine whether the focusing tube is defective when the orifice is defective at the same time. In E3, a non-uniform drop-off can be determined in comparison to E1. Moreover, it can also be detected that the influence of the defective nozzle on the main AWIJ diameter is rather small.

### **3.2 Thermography emission**

The thermographic images show a heating up of the entire cutting head within 60 seconds after switching on the AWIJ (see Figure 6 & 7). After approximately 30 seconds, the system is stable and has reached its respective maximum temperatures. The highest temperatures are reached on the surface of the focus tube with approx. 75 °C followed by safety screw (approx. 60 °C) and mixing chamber (20-35 °C). It can be seen that a defect causes an increase of temperature. On closer examination, it is noticeable that the temperature of the focusing tube in experiment E2 with a deficient orifice is 5 °C lower than in E1 with a new nozzle. It is to be assumed that due to the larger diameter of the damaged orifice more water flows through the orifice and focusing tube so that the water has cooling effect on the focusing tube.

### **3.3 Acoustic emission**

At first, the results of the measurements E1 (green) and E2 (red) were plotted down in Figure 8. The Figure 8a shows the acoustic emission of the new in comparison to the damaged orifice 10 mm above the water line and a pressure of 300 MPa. The signal intensity is plotted on the y axis. The x axis shows the frequency band between 0 and 1000 kHz. In the range between 400 and 1000 kHz, only small signal strengths are measurable. Thus the front range up to 400 kHz was examined more in detail to find a significant frequency which distinguish between new or damaged orifice. By using the mathematical relations (see 2.2.3), the frequency 180 kHz was detected.

Figure 8b with the results of the measurements 10 mm below the water line show nearly the same with a little bit lower signal intensity. This effect is due to the catcher with water, as it acts as a damper. However, a damage to the orifice can also be manifested in this measurement with this experimental setup and the frequency of 180 kHz.

In the next step, the frequency 180 kHz was investigated in the pressure range between 50 and 400 MPa and plotted in Figure 9. The green measuring points stand for the state new and red for the damaged orifice. The signal intensity of the new orifice is higher in all pressure stages than in the damaged ones. This effect is particularly visible at 400 MPa. The graphic shows also no influence if the cutting head is above (Figure 9a) or below (Figure 9b) water line.

In the further investigation of the focusing tube similar effects as for the orifice could be detected. Figure 10 shows the frequency band on the x axis and the signal intensity on the y axis.

Also this graphic shows most differences between new (E1, yellow) and damaged focusing tube (E3, blue) in the frequency range between 50 and 300 kHz. In the same way a weakening of the intensity in the tests below water line can be seen in Figure 10b in comparison to the investigation above the water line (Figure 10a). In order to be able to clearly detect that the focusing tube and not the orifice is broken, a different frequency was chosen. If the signal intensity is considered at the frequency of 163 kHz, a difference between new (E1, yellow) and broken focusing tube (E3, blue) can always be detected with the testing condition 10 mm above water line (Figure 11a). Below the water line this differentiation is not possible (see Figure 11b). It is not possible with this as well as with all other frequencies. The reason for that behavior can be that the sensor is fixed at the mixing chamber and the focus is partly submerged in water, the water in the catcher acts as a vibration damper.

#### **4. CONCLUSIONS & DISCUSSION**

In this study the wear parameters and their influence on the failure of orifices and focusing tubes were studied. The main results can be summarized as follows:

1. It was visually possible to determine that a component is defective in these experiments. However, it is not possible to determine whether it is the focus tube, the orifice or even both components. Meanwhile, the results of the high speed recordings are based on the fact that the WAIS can be observed about a range of 30mm. During cutting the distance between the focusing tube and the work piece is less than 2mm.
2. With the method of thermography emission it can be seen that a defect causes the increase of temperature approx. 5°C in all examined components. However, it is also not possible to determine which component is damaged.
3. High-speed and thermal recording are not possible under water line.
4. It was technically possible to detect a damage of the orifice or the focusing tube by observation of different frequencies with acoustic emission at this experimental setup especially this cutting head. A damage detection was also possible under water line. Only under water line it is very difficult to differentiate between new and damaged focusing tube using this method, caused by damper effect of the water.
5. It is possible to switch within seconds between pure water jet, abrasive water injection jet (AWIJ) and abrasive water suspension jet (AWSJ) by using the design of an automated high pressure screw connection tool.

All in all this study shows the possibility of a full automated cutting with acoustic emission tool monitoring in addition with an automated high pressure screw connection tool without a machine operator.

The next steps in this will be investigations with other types of cutting heads. With this information it will be possible to make a study by a dynamic moving cutting head. In the end there is the vision

of an online observation process, which give the control the signal to change a cutting head because of a damaged component.

## 5. ACKNOWLEDGEMENTS

The whole idea of this design of a full automatized high pressure screw connection tool with a tool monitoring is described in the patent application pending DE102017100183.2.

The authors are members of the Waterjet Laboratory Hannover (WLH, Institut für Werkstoffkunde (Materials Science), Division Underwater Technology Center) and the German Working Group of Waterjet Technology (AWT).

Finally, a special thanks goes to our college student Danny Schickedantz for support this study.

## 6. REFERENCES

- [BAU14] Bauer, M.; Eiben, F.; Bach, Fr.-W.; Maier, H. J.; Hassel, T.: New valve technology for AWSJ cutting, Proceedings of the 22nd International Conference on Water Jetting, Haarlem, Netherlands, 3-5 September 2014, pp. 99-106, 2014.
- [BEC01] Beck, R.; Dempster, A. G.; Kale, I.: Finite-precision Goertzel filters used for signal tone detection. In: IEEE Transactions on Circuits and Systems II: Analog and Digital Signal Processing; Vol. 48 (2001), No. 7, pp. 691–700, 2001.
- [COO65] Cooley, J. W.; Tukey, J. W.: An algorithm for the machine calculation of complex Fourier series. In: Mathematics of Computation; Vol. 19; No. 90; pp. 297-301; 1965.
- [GEN69] Gentleman, W. M.: An error analysis of Goertzel's (Watt's) method for computing Fourier coefficients. In: The Computer Journal; Bd. 12; No. 2; pp. 160-164; 1969.
- [GMA14] GMA Garnet Mesh 120 data sheet: The most popular Waterjet cutting abrasive worldwide - near you!, GMA Garnet (Europe) Hamburg, Hanseatic Trade Center, Hamburg, Germany, 2014.
- [HAS87] Hashish, M.: Wear in abrasive-waterjet cutting systems. In: Ludema K C (ed) 1987 Wear of Materials; Vol. 2; ASME; New York; pp 769-776; 1987.
- [HAS94] Hashish, M.: Observations on wear of abrasive-waterjet nozzle materials. ASME J. of Tribol; 116: 439-444; 1994.
- [KAM02] Kammeyer, K.-D.; Kroschel, K.: Digitale Signalverarbeitung. Wiesbaden: Vieweg+Teubner Verlag, ISBN 978-3-519-46122-7, 2002
- [KEN17] Kennametal data sheet: Roctec Composite Carbide, World Headquarters Kennametal Inc., Latrobe, USA, 2017.
- [KOV89] Kovacevic R.; Beardsley, H.: Nozzle wear sensing in turning operation with abrasive waterjet. In: Proc. Conf. on Nontrad. Machining; SME MS89-809; Soc. of Manuf. Engrs.; Dearborn; pp 1-11; 1989.
- [KOV94] Kovacevic, R.; Wang, L.; Zhang, Y. M.: Identification of abrasive waterjet nozzle wear based on parametric spectrum estimation of acoustic signals. Proc. Inst. Mech. Etzgrs; Journal of Engineering Manufacture; 208: 173-181; 1994.



- [MOM98] Momber, A.W.; Kovacevic, R.: Principles of abrasive water jet machining. Springer-Verlag Berlin Heidelberg New York; 1998.
- [VET84] Vetterli, M.; Nussbaumer, H. J: Simple FFT and DCT algorithms with reduced number of operations. In: Signal processing Bd. 6 (1984), No. 4, pp. 267-278, 1984.

## 7. TABLES

**Table 1.** Mineral composition of GMA Garnet Mesh 120 [GMA14]

<b>Mineral Composition</b>	<b>wt.-%</b>
Garnet (Almandine)	97 - 98
Ilmenite	1 - 2
Zircon	0.20
Quartz (free silica)	<0.5
Others	0.25

**Table 2.** Testing matrix of the experimental setups

	<b>new focusing tube</b>	<b>damaged focusing tube</b>
<b>new orifice</b>	Experimental setup E1	Experimental setup E3
<b>damaged orifice</b>	Experimental setup E2	Experimental setup E4

## 8. NOMENCLATURE

E1 ... E4	Experimental setup 1 ... 4
FFT	Fast fourier transformation
WLH	Waterjet Laboratory Hannover

## 9. GRAPHICS

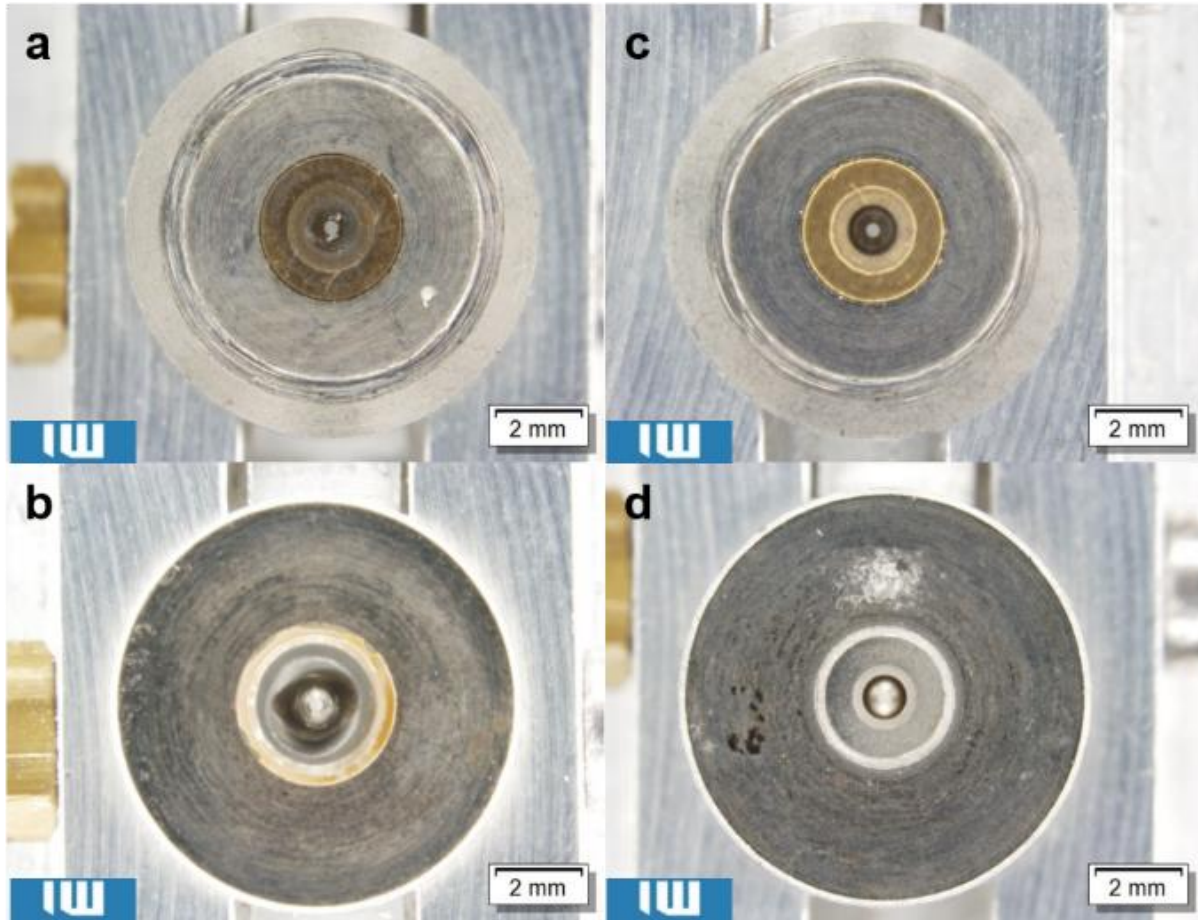


**Figure 1.** Light microscopic images of a damaged (a: top, b: bottom) and a new orifice (c: top, d: bottom) of the orifice type 1830

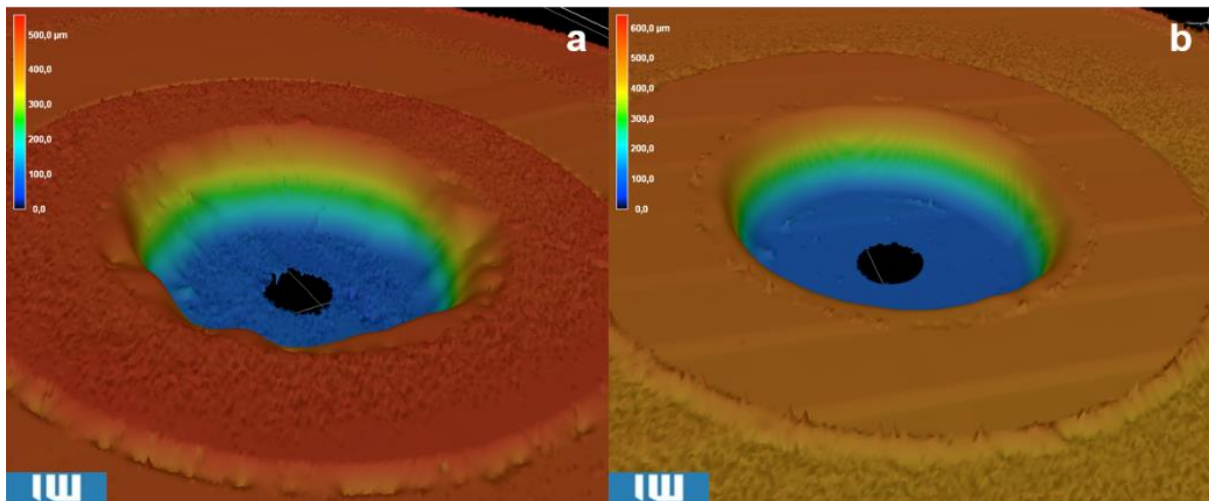


**Figure 2.** Laser confocal microscopic images of the top side of a damaged (a) and a new orifice (b)

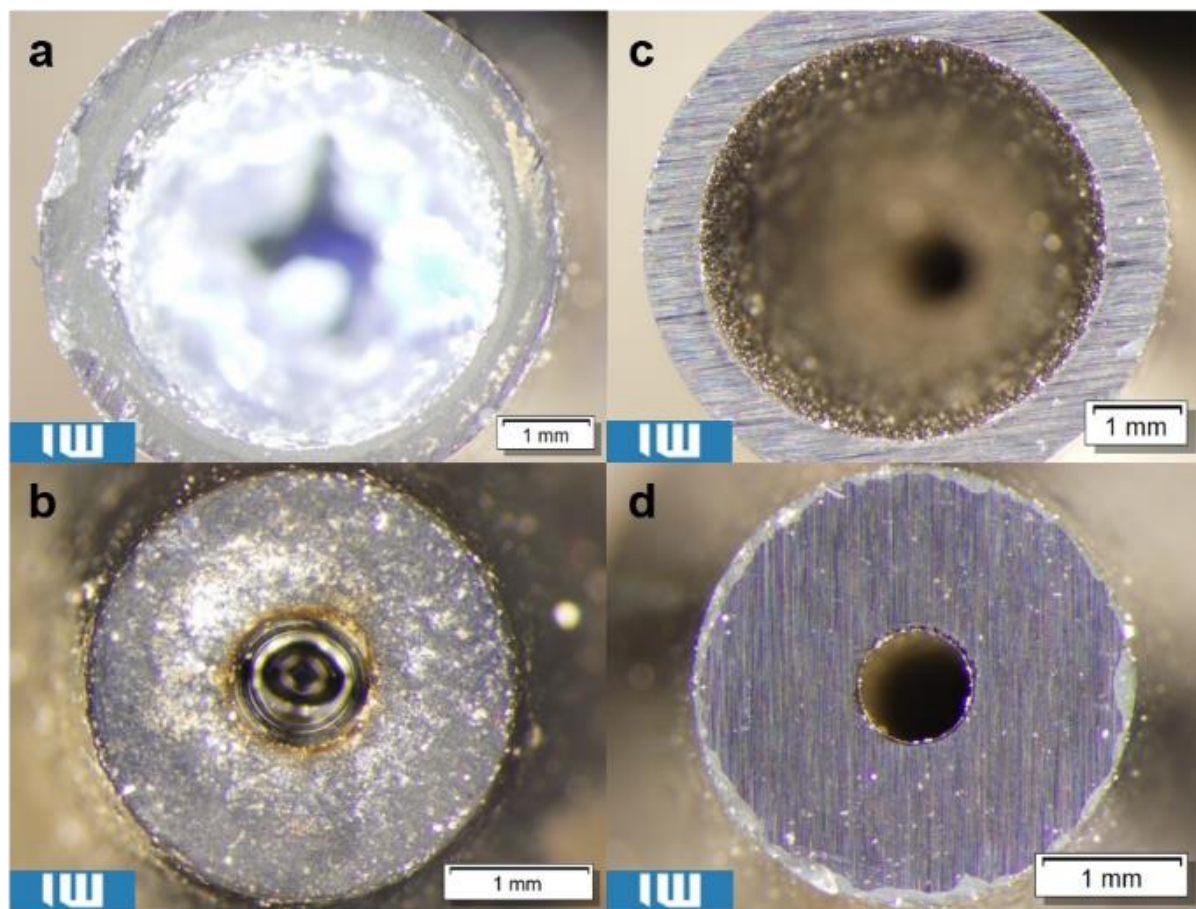
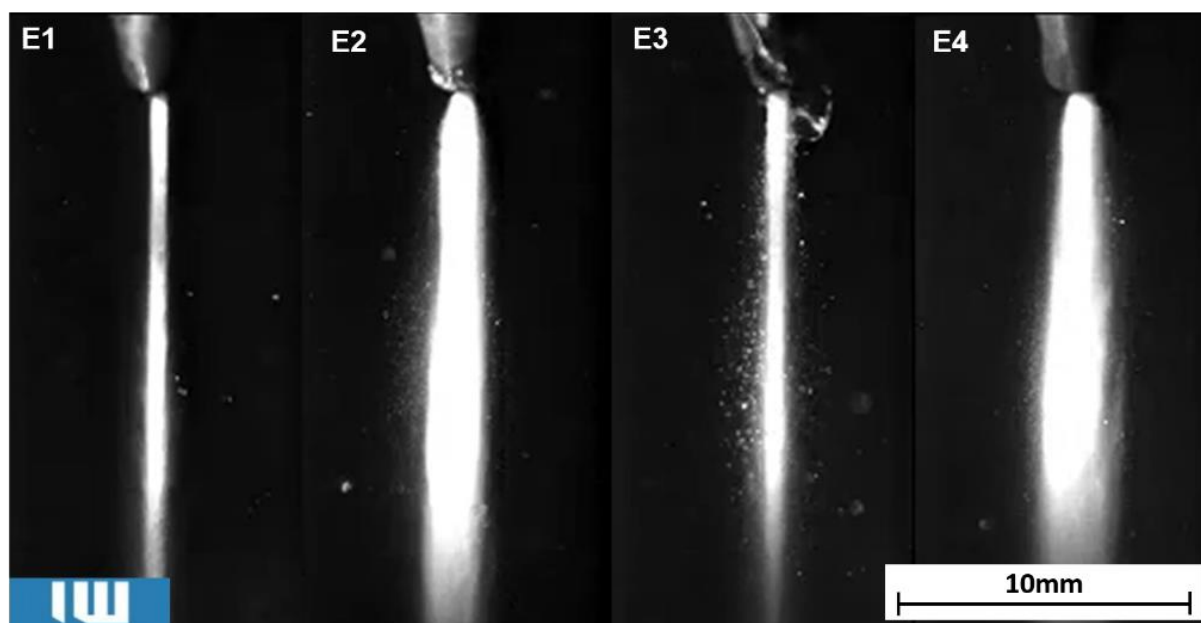


**Figure 3.** Light microscopic images of a damaged (a: top, b: bottom) and a new focusing tube (c: top, d: bottom) of the type Kennametal Roctec 100 6.00x0.8x70mm



$p = 300 \text{ MPa}$ ; abrasive flow 400 g/min

**Figure 4.** High speed recordings –  $p = 300 \text{ MPa}$

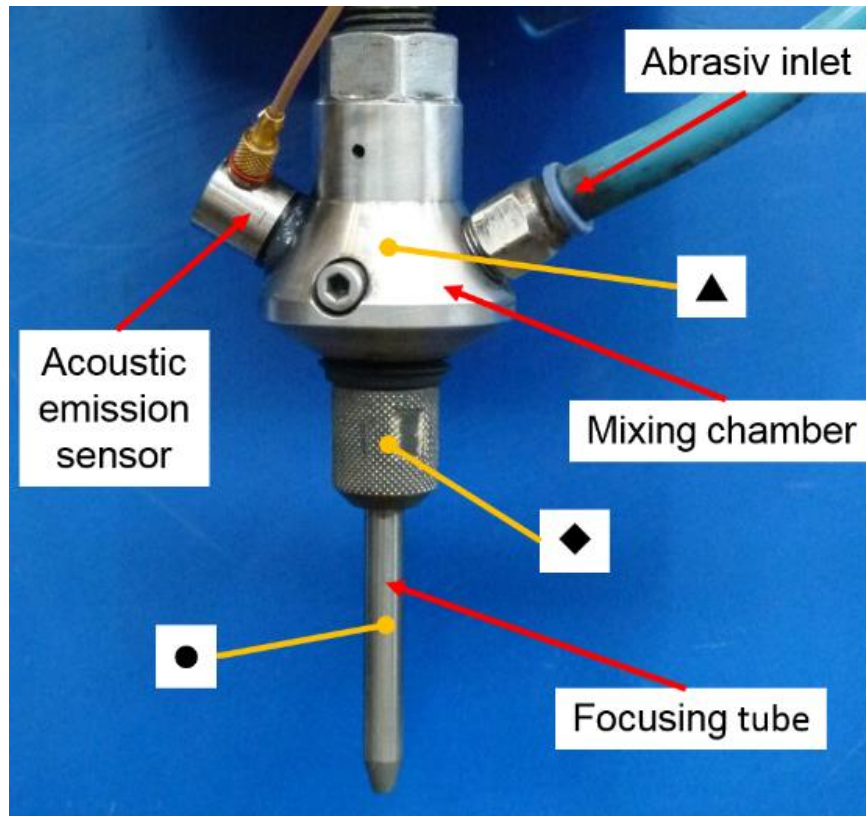
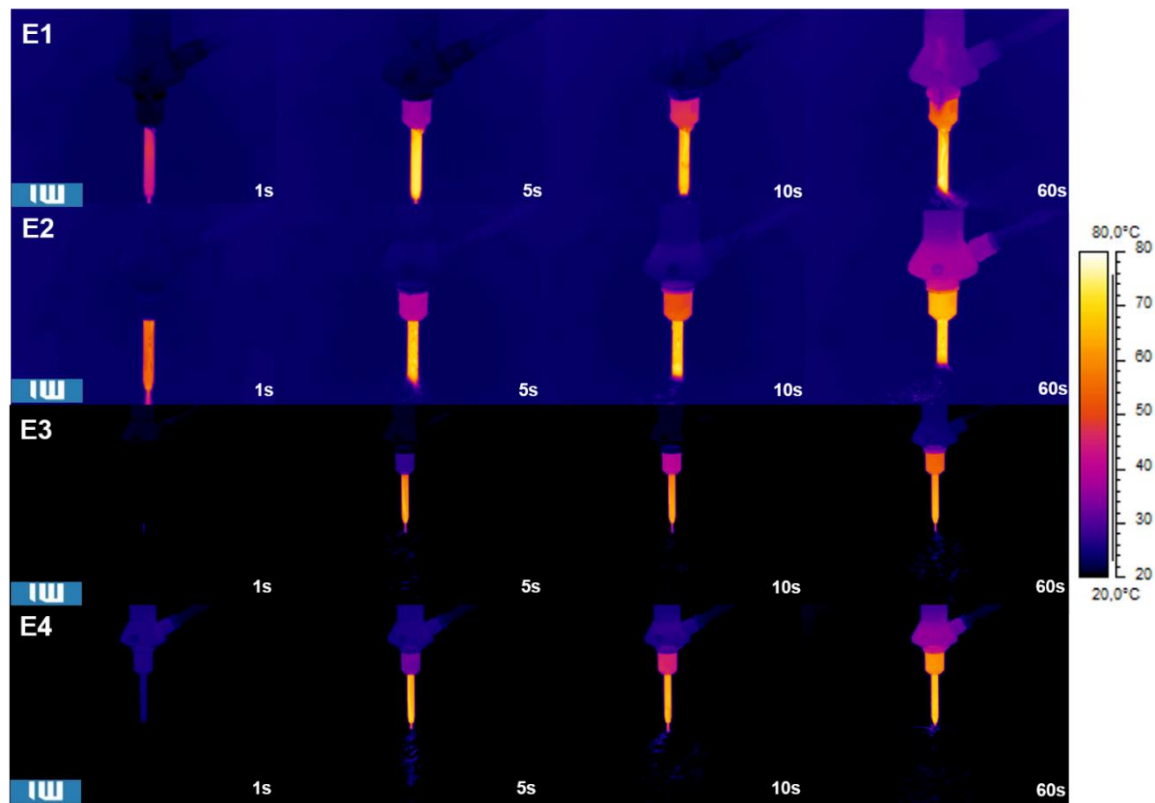


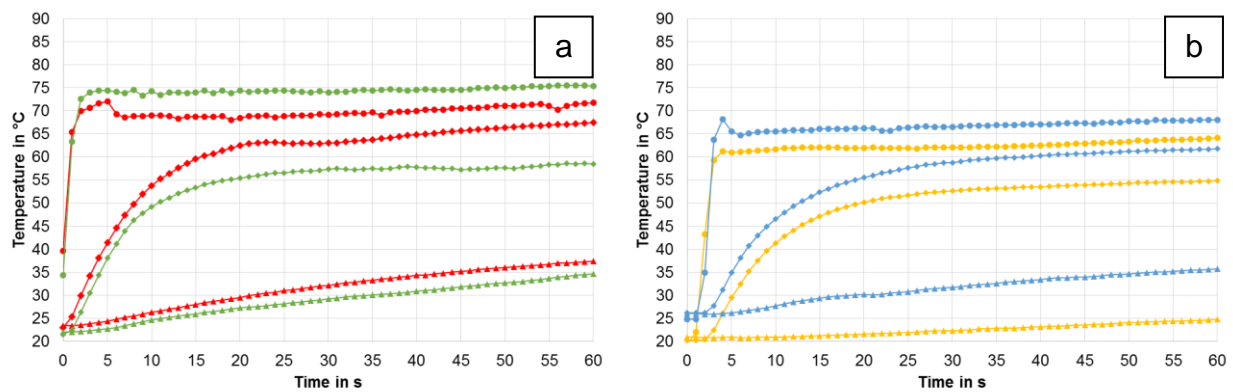
**Figure 5.** Technical setup of the cutting head – Position of the acoustic emission sensor and measuring positions the thermographic investigation (◆ safety screw, ● focusing tube, ▲ mixing chamber)





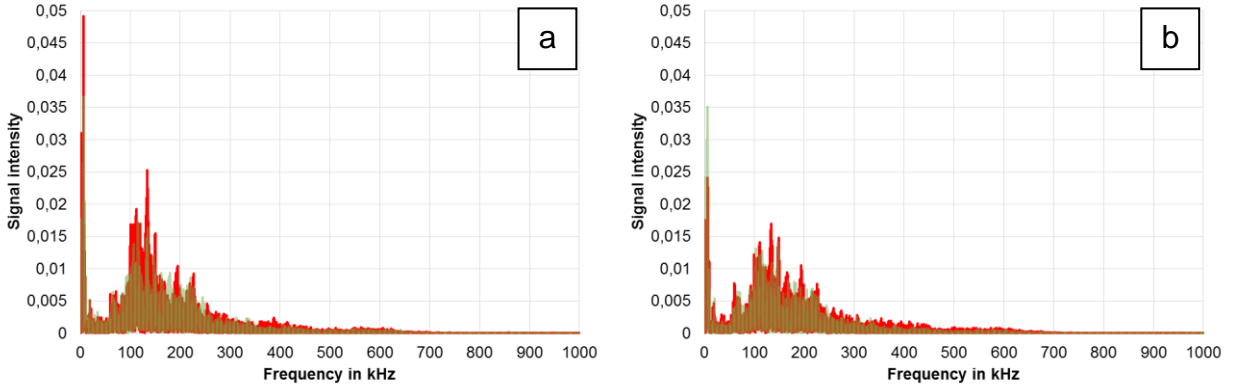
$p = 300 \text{ MPa}$ ; abrasive flow  $400 \text{ g/min}$

**Figure 6.** Thermographic images of the cutting head



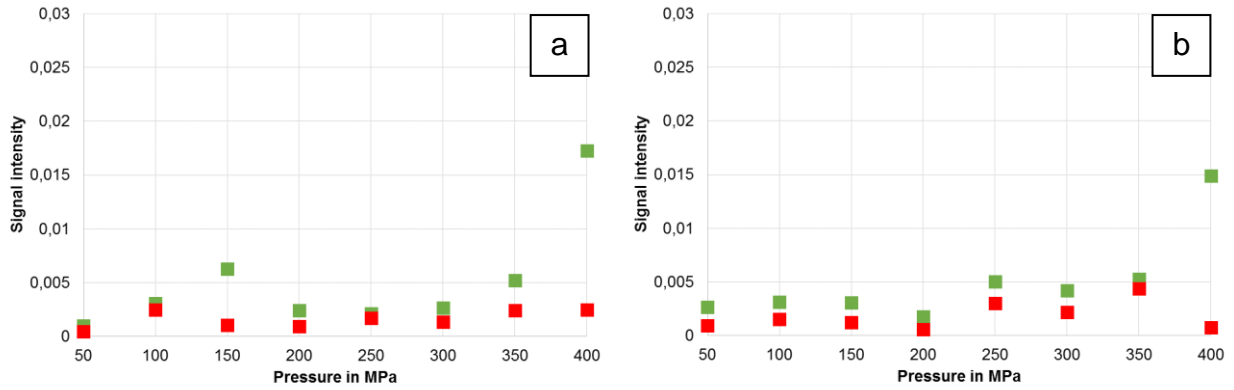
safety screw ◆, focusing tube ● and mixing chamber ▲;  $p = 300 \text{ MPa}$ ; abrasive flow  $400 \text{ g/min}$

**Figure 7.** Cutting heads maximum of temperature – a: E1 (green) vs. E2 (red); b: E3 (yellow) vs. E4 (blue)



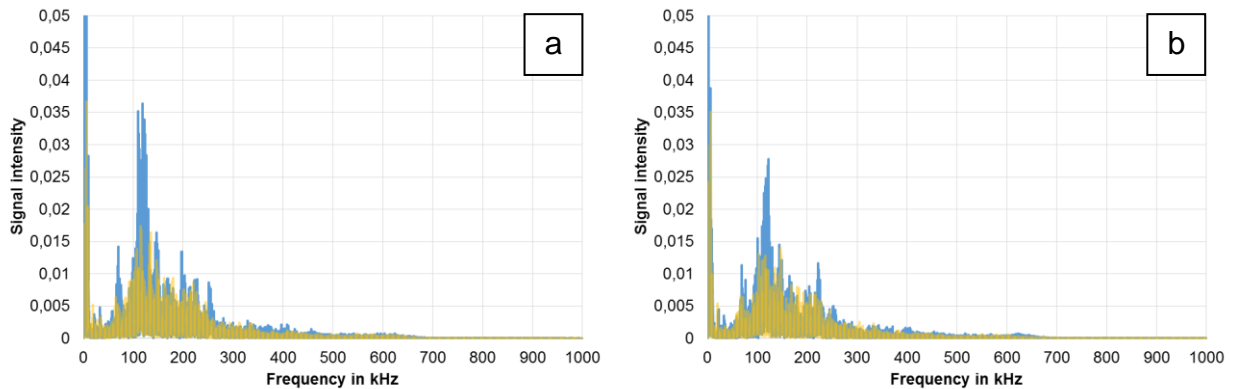
(a) 10 mm over water line, (b) 10 mm under water line;  $p = 300$  MPa; abrasive flow 400 g/min

**Figure 8.** FFT spectra of cutting head's acoustic emission – E1 (green) and E2 (red)



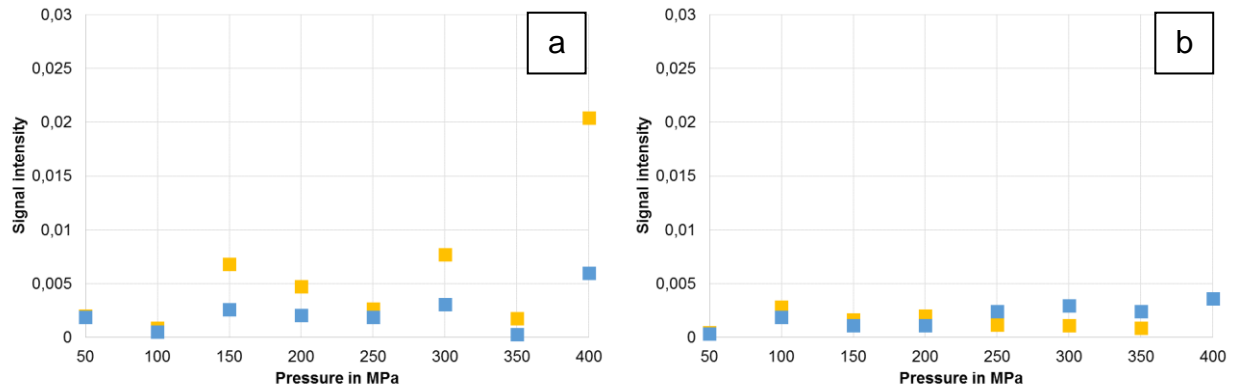
(a) 10 mm over water line, (b) 10 mm under water line; abrasive flow 400 g/min

**Figure 9.** Comparison of cutting head's acoustic emission at different pressures with the significant frequency of 180 kHz – E1 (green) and E2 (red)



(a) 10 mm over water line, (b) 10 mm under water line; abrasive flow 400 g/min

**Figure 10.** FFT spectra of cutting head's acoustic emission – E1 (yellow) and E3 (blue)



(a) 10 mm over water line, (b) 10 mm under water line;  $p = 300$  MPa; abrasive flow 400 g/min

**Figure 11.** Comparison of cutting head's acoustic emission at different pressures with the significant frequency of 163 kHz – E1 (yellow) and E3 (blue)

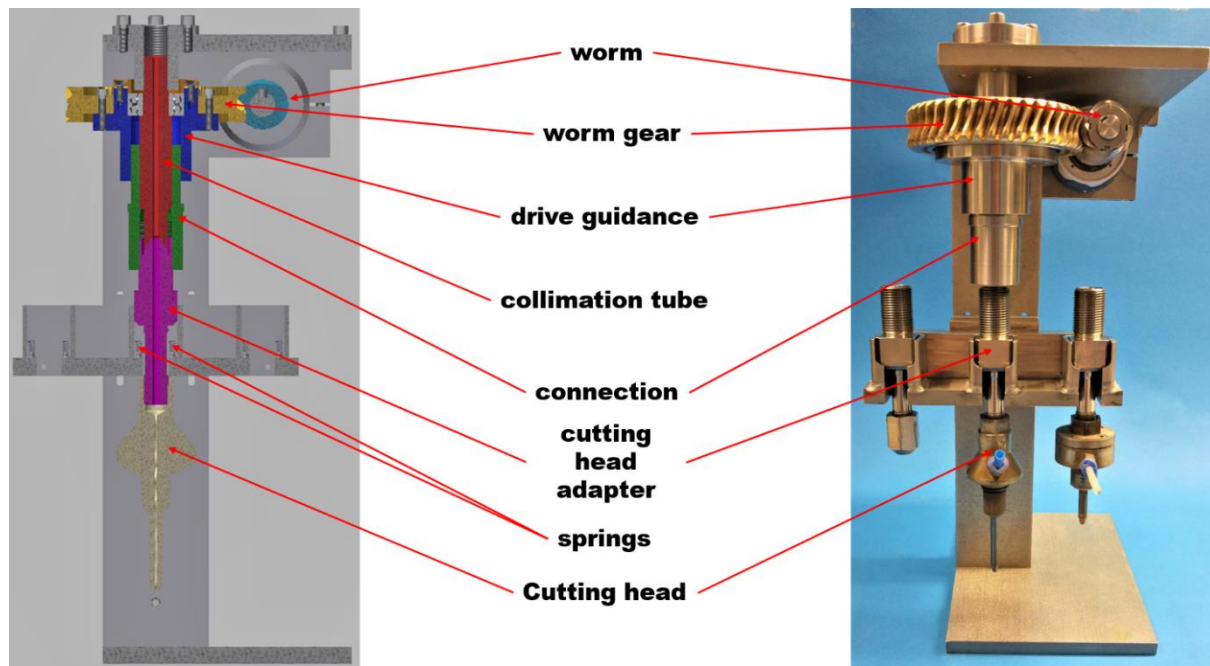


**Figure 12.** Schematic layout (left) and Physical construction (right) of the automated cutting head